Indenyl Carbametallaboranes. Part 2.[1] Compounds with Phenyl or Ether Groups substituted at Cage Carbon Atoms within a 3-(η-C_9H_7)-3,1,2-*closo*-CoC_2B_9 Framework†

Zoë G. Lewis, David Reed and Alan J. Welch *
Department of Chemistry, University of Edinburgh, Edinburgh EH9 3JJ, UK

Reaction of [Co(acac)$_3$] (acac = acetylacetonate), Li[C_9H_7] and $Tl_2[C_2B_9H_9R^1R^2]$ in tetrahydrofuran (thf) affords the substituted indenyl carbacobaltaboranes [1-R^1-2-R^2-3-(η-C_9H_7)-3,1,2-*closo*-$CoC_2B_9H_9$] (R^1 = Ph, R^2 = H **2**; R^1 = CH_2OMe, R^2 = H **3**; R^1 = R^2 = CH_2OMe **4**). The indenyl ligand of **4** (and also, by inference, that of **3**) is, in solution, in rapid rotation about the metal–carbaborane cage axis, even at 185 K. In contrast, the room-temperature solution fluxionality of **2**, which involves synchronous rotation of the indenyl ligand as in **3** and **4** with rotation of the phenyl group about the phenyl–C(1) axis, may be arrested by cooling to 185 K. The limiting low-temperature structure of **2** is in full agreement with the molecular conformation determined in the solid state. For both compounds **2** and **3**, cisoid conformations are observed, in which the ring-junction atoms of the indenyl ligand are as near as they can be to the carbaborane carbon atoms, given an overall staggered relationship between metal-bonded η^5 rings. In contrast the steric influence of two substituent ether functions in **4** is sufficient to push round the six-membered ring of the indenyl ligand to the next best staggered conformation. All the molecular conformations observed, and the relative heights of the barriers to indenyl rotation, are supported by the results of molecular orbital calculations at the extended-Hückel level. Crystal structure data at 185 ± 1 K: **2**, a = 17.732(11), b = 13.186(3), c = 17.739(7) Å, β = 117.00(4)°, space group $C2/c$, R = 0.0439 for 2741 observed reflections; **3**, a = 12.382(3), b = 8.914(5), c = 15.523(9) Å, β = 103.60(4)°, space group $P2_1/c$, R = 0.0269 for 2651 reflections; **4**, a = 10.927(4), b = 14.743(4), c = 11.789(6) Å, β = 90.61(4)°, space group $P2_1/n$, R = 0.0290 for 3087 reflections.

Recently[1] we reported the synthesis and molecular structure of the first indenyl carbametallaborane, [3-(η-C_9H_7)-3,1,2-*closo*-$CoC_2B_9H_{11}$] **1**, an analogue of the cyclopentadienyl compound [3-(η-C_5H_5)-3,1,2-*closo*-$CoC_2B_9H_{11}$] which had been known for some time.[2] Compound **1** and its derivatives are of interest because formal replacement of the η-C_5H_5 ligand by indenyl introduces the possibility of a preferred molecular conformation (indenyl ligand *versus* carbaborane ligand) and of slipping distortions in both η-bonded ligands.[1,3–5]

The results of extended-Hückel molecular orbital (EHMO) calculations on an idealised model of compound **1** suggested that the preferred conformation was that in which the indenyl ring-junction carbon atoms lay cisoid ('cisoid' implies a *cis*-staggered arrangement of the two η-bonded rings) to the cage carbon atoms, and such a conformation was indeed observed crystallographically (see later). Clearly, therefore, substitution at one or both cage carbon atoms by bulky alkyl or aryl functions could result in competing electronic and steric effects on the preferred conformation. In this paper we accordingly report the synthesis and structural characterisation of two mono- and one di-substituted derivatives of **1**.

Experimental

Syntheses.—All reactions were performed under an atmosphere of dry, oxygen-free N_2 using standard Schlenk-line techniques, with some subsequent manipulation in air. Solvents were dried and distilled under N_2 prior to use. Infrared spectra were recorded as CH_2Cl_2 solutions on a Perkin-Elmer 598 spectrophotometer, and NMR spectra, unless otherwise stated, as CD_2Cl_2 solutions at room temperature on a Bruker WH360 spectrometer. Chemical shifts are reported relative to external $SiMe_4$ (^{1}H) or BF_3·OEt_2(^{11}B), with positive shifts to high frequency in each case.

The compounds Tl_2[7-Ph-7,8-*nido*-$C_2B_9H_{10}$],[6] Tl_2[7-CH_2-OMe-7,8-*nido*-$C_2B_9H_{10}$][7] and Tl_2[7,8-$(CH_2OMe)_2$-7,8-*nido*-$C_2B_9H_9$][7] ‡ were synthesised as described previously, Li[C_9H_7] was prepared from freshly distilled indene (BDH) and LiBu (Aldrich) in tetrahydrofuran (thf), and [Co(acac)$_3$] (acac = acetylacetonate) (Koch-Light) was used as supplied.

[1-Ph-3-(η-C_9H_7)-3,1,2-*closo*-$CoC_2B_9H_{10}$] **2**. The complex [Co(acac)$_3$] (0.52 g, 1.46 mmol) was dissolved in thf, and Tl_2[7-Ph-7,8-*nido*-$C_2B_9H_{10}$] (0.90 g, 1.46 mmol) was suspended in the resulting green solution. The mixture was stirred at room temperature and to it was added, dropwise, a freshly prepared solution of Li[C_9H_7] (1.46 mmol) in thf. The resultant brown product was stirred overnight and filtered. Volatiles were removed from the filtrate *in vacuo*, and the resultant solid dissolved in CH_2Cl_2 (15 cm^3) and filtered. The filtrate was concentrated and chromatographed on silica plates using hexane–CH_2Cl_2 (1:1) as eluent. Yellow (R_f 0.9, no B–H by IR spectroscopy) and orange (R_f 0.7, B–H containing) bands were collected, the latter obtained as a dark red *solid* from CH_2Cl_2 and subsequently identified as [1-Ph-3-(η-C_9H_7)-3,1,2-*closo*-

† *Supplementary data available:* see Instructions for Authors, *J. Chem. Soc., Dalton Trans.*, 1992, Issue 1, pp. xx–xxv.
Non-SI unit employed: eV ≈ 1.60 × 10^{-19} J.

‡ These three compounds are written as 2:1 salts but may ultimately prove to be better represented as 1:1 salts in which one Tl^+ is (albeit weakly) associated with the carbaborane dianion.[8]

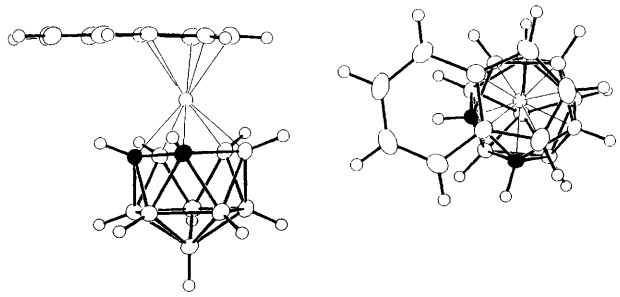

Perspective and plan views of compound **1** (cage carbon atoms black)

$CoC_2B_9H_{10}$] **2**. Yield 10% (Found: C, 53.2; H, 5.70. $C_{17}H_{22}B_9Co$ requires C, 53.4; H, 5.80%); ν_{max} 2540 cm^{-1} (B–H). NMR: ^{11}B-{^1H}, δ 8.25 (1 B), 2.34 (1 B), −2.73 [2B (coincident)], −3.62 (1 B), −6.32 (1 B), −11.00 (1 B), −16.74 (1 B) and −17.72 (1 B); the ^1H chemical shifts are presented and discussed in the text.

[1-CH_2OMe-3-(η-C_9H_7)-3,1,2-*closo*-$CoC_2B_9H_{10}$] **3**. Similarly, [Co(acac)$_3$], Tl_2[7-CH_2OMe-7,8-*nido*-$C_2B_9H_{10}$] and Li[C_9H_7] (1.72 mmol of each) were allowed to react to afford, after work-up involving preparative TLC, [1-CH_2OMe-3-(η-C_9H_7)-3,1,2-*closo*-$CoC_2B_9H_{10}$] **3** as dark red *microcrystals*. Yield 5% (Found: C, 44.1; H, 6.20. $C_{13}H_{22}B_9CoO$ requires C, 44.5; H, 6.35%); ν_{max} 2530 cm^{-1} (B–H). NMR: ^{11}B-{^1H}, δ 8.69 (1 B), 1.68 (1 B), −2.65 (1 B), −3.54 (1 B), −4.58 (1 B), −7.00 (1 B), −12.46 (1 B), −17.58 (1 B) and −19.94 (1 B): ^1H, δ 2.52 [s, 1 H, H(2)], 3.53 (s, 3 H, CH_3), 3.61 and 3.72 (AB, $^2J_{HH}$ 11, 2 H, $-CH_2O$], 5.66 [d of d (app. t), $^3J_{HH}$ 3, 3, 1 H, H(32)], 6.39 [d, $^3J_{HH}$ 3 Hz, 2 H (coincident), H(31, 32)] and 7.44–7.61 [m, 4 H, H(35–38)].

[1,2-$(CH_2OMe)_2$-3-(η-C_9H_7)-3,1,2-*closo*-$CoC_2B_9H_9$] **4**. The complex [Co(acac)$_3$], Tl_2[7,8-$(CH_2OMe)_2$-7,8-*nido*-$C_2B_9H_9$] and Li[C_9H_7] (0.86 mmol of each) were allowed to react together as described above, except that the reaction was judged to be complete after only 2.5 h, to afford, after work-up involving preparative TLC [1,2-$(CH_2OMe)_2$-3-(η-C_9H_7)-3,1,2-*closo*-$CoC_2B_9H_9$] **4** as a dark red *solid*. Yield 12% (Found: C, 45.8; H, 6.60. $C_{15}H_{26}B_9CoO_2$ requires C, 45.7; H, 6.65%); ν_{max} 2540 cm^{-1} (B–H). NMR: ^{11}B-{^1H}, δ 8.93 (1 B), 1.86 (1 B), −1.65 (2 B), −5.15 (2 B), −14.19 (2 B) and −17.89 (1 B): ^1H, δ 3.17 and 3.39 (AB, $^2J_{HH}$ 12, 4 H, CH_2O), 3.34 (s, 6 H, CH_3), 5.70 [t, $^3J_{HH}$ 3, 1 H, H(32)], 6.40 [d, $^3J_{HH}$ 3 Hz, 2 H, H(31, 32)] and 7.51–7.58 [m, 4 H, H(35–38)].

Crystallographic Studies.—Diffraction-quality crystals of compounds **2–4** were grown by diffusion of hexane into CH_2Cl_2 solutions at 243 K.

All crystallographic measurements were made at 185 ± 1 K on an Enraf-Nonius CAD4 diffractometer equipped with Mo-Kα X-radiation, $\bar{\lambda}$ = 0.710 69 Å, and a ULT-1 nitrogen-gas cooling device. Orientation matrix and unit-cell parameters by least-squares refinement of the setting angles of 25 high-angle reflections. Data collection in the range $1 \leqslant \theta \leqslant 25°$ at variable speeds by ω–2θ scans in 96 steps with ω scan width 0.8 + 0.34 tan θ. One asymmetric fraction of data ($+h + k \pm l$) was measured in each case, and for **2** only data with $(h + k) = 2n$.

Data from compound **2** were corrected for slight decay and all data reduced by CADABS.[9] The cobalt positions were found by direct methods[10] and those of all other atoms by iterative full-matrix least-squares refinement/ΔF syntheses.[11] After isotropic convergence an empirical absorption correction was applied.[12] In the final stages of refinement reflections were weighted according to $w^{-1} = \sigma^2(F) + gF^2$. All non-hydrogen atoms were allowed anisotropic thermal motion. For **2**, H atoms of the phenyl ring and indenyl ligand were set in idealised positions and cage H atoms refined with tied C–H/B–H distances, 1.10(2) Å at convergence; all H atoms in this structure refined with a common isotropic thermal parameter. For **3** and **4** all H atoms freely refined with individual isotropic thermal parameters.

General crystallographic data, details of data collection and of structure refinement, are given in Table 1. Tables 2–4 list coordinates of refined atoms for compounds **2–4** respectively. Computer programs used in addition to those referenced above: CALC[13] and EASYORTEP.[14]

Additional material available from the Cambridge Crystallographic Data Centre comprises H-atom coordinates, thermal parameters and remaining bond lengths and angles.

EHMO Calculations.—The EHMO calculations were performed on idealised models of compounds **1–4** varying α, the angle describing the conformation of the indenyl six-membered ring relative to the cage carbon atoms,[1] using a local version of the program ICON 8[15] and the modified Wolfsberg–Helmholtz formula.[16] The H_{ii} values for C, B and H and Slater exponents for all elements (double zeta for Co) were those inlaid in ICON 8, whilst H_{ii} for Co were initially optimised by charge iteration (using nine valence shell ionisation energy functions) on model compound **1** in the *cis*-eclipsed conformation (α = 0°), affording 3d −12.075, 4s −9.128 and 4p −5.515 eV. Table 5 details parameters used to construct the models.

Results and Discussion

Compounds **2–4**, C-cage substituted derivatives of [3-(η-C_9H_7)-3,1,2-*closo*-$CoC_2B_9H_{11}$] **1**, have been synthesised by an analogous route to that which has previously afforded **1**[1] and [3-(η-C_5H_5)-3,1,2-*closo*-$CoC_2B_9H_{11}$].[2] Although yields of these new compounds, after work-up involving preparative TLC, are low (5–15%), all are afforded in high purity. The compounds are stable to air for long periods in solution, and indefinitely in the solid state.

Compounds **3** and **4** (the mono- and di-ether derivatives respectively) were characterised by microanalysis, IR and ^1H, ^{11}B and ^{11}B-{^1H} NMR spectroscopy. In the ^1H NMR spectra the CH_2 group of the pendant ether function gives rise to an AB pattern with $^2J_{HH}$ 11 (**3**) and 12 Hz (**4**). All resonances in the ^{11}B NMR spectra show the expected doublet coupling, $^1J_{BH}$ 120–155 Hz. Both the ^{11}B and ^{11}B-{^1H} NMR spectra of **4** are consistent with time-averaged C_s molecular symmetry, and are unchanged on cooling to 185 K. In view of the preference for a molecular conformation which does not have mirror symmetry (see later), these spectra can only be interpreted in terms of facile rotation of the indenyl ligand about the metal–cage axis, even at low temperature. Note, however, that distinction cannot be made between full and partial rotation. It is likely that similar fluxionality occurs in **3**.

At 298 K the ^1H NMR spectrum of compound **2** (the monophenyl derivative) contains resonances due to H(2) (δ 2.52) and seven indenyl protons, but only three phenyl protons. Owing to this anomaly the high-frequency region of the spectrum has been monitored as a function of decreasing temperature, the results of which are presented in Fig. 1. Table 6 lists ^1H assignments at 298 and 185 K. All except those of H(12), H(13), H(15) and H(16) are based on a series of selective decoupling experiments carried out at 298 K; H(13) and H(15) were distinguished as a result of decoupling H(16) at 185 K, and there is one coincidence at 185 K, δ *ca.* 7.3, involving H(13) and H(14) (see Fig. 3 for atom labelling and preferred molecular conformation). Although H(12) and H(16) are not observed at 298 K, broad signals due to these two atoms begin to appear at 264 K, and by 223 K each has been resolved into a doublet. In addition, the signal due to H(13) and H(15) broadens at 264 K and is resolved into two distinct resonances at lower temperatures.

These observations are consistent with rapid rotation of the phenyl ring about the C(1)–C(11) axis at room temperature becoming restricted on cooling. Moreover, as the temperature is

Table 1 Crystallographic data and details of data collection and structure refinement

	$C_9H_7CoC_2B_9H_{10}Ph$ **2**	$C_9H_7CoC_2B_9H_{10}(CH_2OMe)$ **3**	$C_9H_7CoC_2B_9H_9(CH_2OMe)_2$ **4**
Formula	$C_{17}H_{22}B_9Co$	$C_{13}H_{22}B_9CoO$	$C_{15}H_{26}B_9CoO_2$
M	382.59	350.54	394.58
System	Monoclinic	Monoclinic	Monoclinic
Space group	$C2/c$	$P2_1/c$	$P2_1/n$
a/Å	17.732(11)	12.382(3)	10.927(4)
b/Å	13.186(3)	8.914(5)	14.743(4)
c/Å	17.739(7)	15.523(9)	11.789(6)
β/°	117.00(4)	103.60(4)	90.61(4)
U/Å^3	3695	1665	1899
Z	8	4	4
D_c/g cm^{-3}	1.375	1.398	1.380
μ(Mo-Kα)/cm^{-1}	9.22	10.21	9.06
F(000)	1568	700	816
θ/° (orientation)	12–16	14–16	14–16
Scan speed/° min^{-1}	0.79–2.35	0.79–2.35	0.82–2.06
Data collection time/h	99	85	89
Crystal decay (%)	8	None	None
Unique data	2768	2654	3094
Observed' data [$F \geqslant 2\sigma(F)$]	2741	2651	3087
H Atoms	Aromatic H set in idealised positions; cage H refined with common X–H distance	Freely refined	Freely refined
U_H/Å^2	0.0434(23)	0.021(5)–0.102(13)	0.014(5)–0.078(11)
g	0.000 303	0.002 296	0.001 416
No. of variables	276	305	348
R	0.0439	0.0269	0.0290
R'	0.0525	0.0428	0.0488
S	1.293	0.832	1.169
Maximum, minimum residues/e Å^{-3}	0.20, −0.20	0.24, −0.47	0.29, −0.57

Table 2 Coordinates of refined atoms for compound **2**

Atom	x	y	z
C(1)	0.247 92(20)	0.322 81(24)	0.283 58(20)
C(2)	0.307 18(21)	0.415 53(25)	0.276 90(20)
Co(3)	0.307 72(3)	0.292 05(3)	0.210 93(3)
B(4)	0.306 44(25)	0.212 9(3)	0.310 07(24)
B(5)	0.288 6(3)	0.283 1(3)	0.386 92(24)
B(6)	0.287 9(3)	0.412 5(3)	0.363 73(24)
B(7)	0.406 71(25)	0.377 8(3)	0.297 32(25)
B(8)	0.410 4(3)	0.246 1(3)	0.321 95(25)
B(9)	0.390 6(3)	0.235 6(3)	0.411 8(3)
B(10)	0.378 9(3)	0.360 1(3)	0.444 67(25)
B(11)	0.387 2(3)	0.446 9(3)	0.373 12(25)
B(12)	0.453 0(3)	0.338 6(3)	0.404 7(3)
C(11)	0.153 09(20)	0.328 6(3)	0.233 16(19)
C(12)	0.110 82(22)	0.420 1(3)	0.207 41(21)
C(13)	0.023 83(24)	0.423 2(4)	0.162 88(22)
C(14)	−0.022 76(24)	0.334 5(4)	0.142 59(22)
C(15)	0.018 73(25)	0.242 3(4)	0.167 54(22)
C(16)	0.106 86(23)	0.238 6(3)	0.213 40(21)
C(31)	0.358 82(23)	0.270 9(3)	0.130 57(21)
C(32)	0.317 71(24)	0.181 3(3)	0.137 06(22)
C(33)	0.231 09(23)	0.202 6(3)	0.109 38(20)
C(34)	0.216 22(22)	0.305 8(3)	0.080 28(19)
C(35)	0.141 9(3)	0.365 5(3)	0.047 13(22)
C(36)	0.149 7(3)	0.464 2(4)	0.029 26(24)
C(37)	0.227 0(3)	0.506 4(3)	0.041 3(3)
C(38)	0.300 8(3)	0.451 1(3)	0.073 69(24)
C(39)	0.295 75(23)	0.347 7(3)	0.093 11(20)

lowered, the resonances due to H(12) and H(35), marked * and † respectively on Fig. 1, move to progressively lower frequency. This suggests that the restricted rotation of the phenyl group is enforced by a preferred conformation of the indenyl ligand (Fig. 3) such that H(12) and H(35) experience the magnetic anisotropy of the C(34)–C(39) and C(11)–C(16) ring systems respectively. Similarly, the resonance due to H(2) moves from δ 2.51 at 298 K to 2.39 at 264 K, 2.23 at 223 K and 2.08 at 185 K as it is progressively located under C(34)–C(39). In summary, the conformation ultimately observed in the solid state (and shown to be electronically preferred, see later) is fully consistent with the limiting low-temperature solution structure.

Compounds **2**–**4** all afford excellent single crystals, and accurate diffraction data were collected from each at low temperature (185 ± 1 K), primarily to determine the effects on molecular conformation of progressive cage-carbon substitution of **1**. Fig. 2 presents perspective and plan views of **2**, whilst those for **3** and **4** appear as Figs. 3 and 4 respectively. Table 7 compares selected interatomic distances for **2**–**4**.

The reasons for the electronically preferred molecular conformations of compound **1** and the slipping distortions of both its indenyl and carbaborane ligands have been comprehensively discussed elsewhere[1] and thus will not be restated in full here. Briefly, metal–carbaborane bonding is stronger to the facial boron atoms [B(4)B(8)B(7)] than to the facial carbon atoms [C(1)C(2)] since the frontier molecular orbitals (MOs) of [7,8-*nido*-$C_2B_9H_{11}$]$^{2-}$ are localised on the former.[4] At the same time, metal–indenyl bonding is stronger to the three-atom sequence C(31)C(32)C(33) than to the ring-junction atoms C(34)C(39) since the p_π atomic orbitals of these junction atoms are delocalised over the entire indenyl π system. Overall, therefore, the optimum molecular conformation is that in which strong metal–carbaborane bonding compensates for weak metal–indenyl bonding and *vice versa*, given the constraint of an overall staggered arrangement of metal-bonded five-membered rings, *i.e.* the cisoid conformation of **1**. In **2**–**4** the introduction of bulky substituents at C(1) and C(2) could, therefore, give rise to competing electronic and steric effects.

In compound **2** a single phenyl group is substituted at C(1). Fig. 2 clearly shows that the observed conformation of the indenyl six-membered ring is cisoid with respect to the cage-carbon atoms. Recall that this conformation is in full accord with the limiting low-temperature ^{1}H NMR spectrum of **2**. The phenyl substituent subtends an elevation angle at C(1) of 21.6 [all geometrical calculations involving **1**–**4** are related to the lower pentagonal belt B(5)B(6)B(11)B(12)B(9) which is, in

Table 3 Coordinates of refined atoms for compound **3**

Atom	*x*	*y*	*z*	Atom	*x*	*y*	*z*
Co(3)	0.214 93(2)	−0.017 72(3)	0.300 20(1)	B(12)	0.333 00(18)	−0.316 84(24)	0.240 12(15)
C(31)	0.181 01(18)	−0.044 48(25)	0.420 09(13)	H(2)	0.398 8(17)	0.068(3)	0.285 1(13)
C(32)	0.018 31(19)	−0.017 41(24)	0.354 88(14)	H(4)	0.064 6(18)	−0.074(3)	0.150 7(14)
C(33)	0.088 71(15)	0.123 53(23)	0.316 56(12)	H(5)	0.197 1(19)	−0.077(3)	0.027 1(15)
C(34)	0.191 09(15)	0.192 19(21)	0.361 55(11)	H(6)	0.412 0(18)	0.035 8(23)	0.127 8(14)
C(35)	0.239 84(17)	0.334 45(22)	0.352 08(13)	H(7)	0.383 7(18)	−0.184(3)	0.386 8(15)
C(36)	0.341 40(18)	0.365 84(24)	0.405 37(14)	H(8)	0.151 2(17)	−0.308 3(25)	0.297 6(14)
C(37)	0.398 97(17)	0.260 21(25)	0.468 09(13)	H(9)	0.163 1(21)	−0.369(3)	0.108 5(17)
C(38)	0.356 23(16)	0.124 15(23)	0.479 39(12)	H(10)	0.392 7(20)	−0.301(3)	0.092 9(16)
C(39)	0.249 20(15)	0.086 87(22)	0.426 36(11)	H(11)	0.520 5(19)	−0.172(3)	0.265 0(14)
C(11)	0.228 41(16)	0.187 60(21)	0.149 05(13)	H(12)	0.361 9(17)	−0.433(3)	0.260 6(14)
O	0.115 66(11)	0.229 62(16)	0.134 81(8)	H(31)	0.193 3(19)	−0.125(3)	0.448 7(15)
C(12)	0.054 65(22)	0.213 0(3)	0.045 58(16)	H(32)	0.026 9(21)	−0.070(3)	0.336 2(16)
C(1)	0.249 49(16)	0.024 41(19)	0.180 19(13)	H(33)	0.033 6(17)	0.169 9(25)	0.266 5(14)
C(2)	0.358 72(17)	−0.012 65(20)	0.262 32(14)	H(35)	0.199 3(19)	0.406(3)	0.305 7(15)
B(4)	0.149 78(17)	−0.111 17(23)	0.177 07(13)	H(36)	0.373 0(20)	0.463(3)	0.402 0(16)
B(5)	0.237 79(18)	−0.111 21(25)	0.100 79(14)	H(37)	0.462 6(23)	0.289(3)	0.500 6(15)
B(6)	0.369 55(17)	−0.042 69(25)	0.154 94(14)	H(38)	0.391 7(21)	0.052(3)	0.517 9(16)
B(7)	0.343 18(17)	−0.172 11(24)	0.319 85(14)	H(111)	0.250 1(16)	0.196 9(24)	0.092 7(14)
B(8)	0.209 01(17)	−0.243 87(23)	0.264 93(14)	H(112)	0.270 7(17)	0.251(3)	0.196 3(13)
B(9)	0.213 19(18)	−0.280 2(3)	0.152 67(14)	H(121)	0.079(3)	0.144(4)	0.016 8(21)
B(10)	0.348 65(18)	−0.237 9(3)	0.138 99(15)	H(122)	−0.013 8(25)	0.212(3)	0.046 0(17)
B(11)	0.428 23(17)	−0.168 0(3)	0.241 82(15)	H(123)	0.065(3)	0.308(5)	0.017(3)

Table 4 Coordinates of refined atoms for compound **4**

Atom	*x*	*y*	*z*	Atom	*x*	*y*	*z*
Co(3)	1.039 17(2)	0.187 42(1)	0.203 90(2)	H(4)	1.168 1(18)	0.341 8(14)	0.178 2(17)
C(31)	1.178 34(17)	0.133 23(13)	0.113 20(16)	H(5)	1.020 7(19)	0.460 1(16)	0.293 1(18)
C(32)	1.095 70(19)	0.176 52(14)	0.038 35(17)	H(6)	0.793 5(18)	0.373 1(14)	0.337 9(16)
C(33)	0.979 08(17)	0.135 53(12)	0.048 81(15)	H(7)	0.984 9(17)	0.092 1(13)	0.392 5(16)
C(34)	0.990 84(16)	0.060 41(12)	0.125 68(14)	H(8)	1.244(3)	0.198 5(17)	0.346(3)
C(35)	0.906 47(17)	−0.005 15(13)	0.164 55(16)	H(9)	1.214 5(20)	0.369 0(15)	0.428 5(19)
C(36)	0.946 63(19)	−0.068 59(13)	0.240 57(17)	H(10)	0.975 3(19)	0.397 9(15)	0.523 3(18)
C(37)	1.070 49(19)	−0.070 15(13)	0.280 23(17)	H(11)	0.836 4(20)	0.223 9(16)	0.504 1(19)
C(38)	1.153 87(18)	−0.008 48(13)	0.245 61(16)	H(12)	1.101 9(20)	0.219 8(16)	0.551 2(20)
C(39)	1.115 07(16)	0.059 36(12)	0.166 42(15)	H(31)	1.254 8(22)	0.150 6(17)	0.128 4(19)
C(1)	0.959 74(17)	0.310 65(10)	0.225 92(16)	H(32)	1.116 1(19)	0.226 4(16)	−0.004 5(20)
C(2)	0.894 59(15)	0.226 61(11)	0.300 56(14)	H(33)	0.902 5(22)	0.149 9(16)	−0.000 6(20)
C(11)	0.901 99(18)	0.346 27(13)	0.116 53(16)	H(35)	0.823 7(22)	−0.016 7(17)	0.132 4(21)
O(11)	0.849 41(15)	0.432 46(9)	0.133 19(11)	H(36)	0.893 0(24)	−0.121 3(19)	0.257 8(21)
C(111)	0.802 52(25)	0.469 88(16)	0.031 07(20)	H(37)	1.098 4(18)	−0.125 8(15)	0.326 3(18)
C(21)	0.776 73(17)	0.180 77(12)	0.259 82(17)	H(38)	1.237 9(22)	−0.008 0(16)	0.268 6(19)
O(21)	0.673 70(11)	0.216 09(10)	0.315 14(12)	H(111)	0.837 6(20)	0.302 8(14)	0.084 2(19)
C(211)	0.565 52(19)	0.167 04(17)	0.285 52(20)	H(112)	0.968 6(22)	0.349 2(17)	0.050 6(21)
B(4)	1.117 61(20)	0.310 03(13)	0.245 96(19)	H(211)	0.781 8(19)	0.109 5(16)	0.272 6(18)
B(5)	1.020 49(19)	0.389 72(14)	0.316 22(17)	H(212)	0.768 0(21)	0.183 5(13)	0.183 1(22)
B(6)	0.879 38(19)	0.336 67(14)	0.347 85(17)	H(1A)	0.859(3)	0.472 0(20)	−0.026(3)
B(7)	1.006 36(19)	0.165 31(15)	0.372 84(17)	H(1B)	0.743(3)	0.430 8(24)	0.004(3)
B(8)	1.150 91(18)	0.220 00(14)	0.344 42(17)	H(1C)	0.784 2(23)	0.529 7(20)	0.045 2(21)
B(9)	1.138 31(20)	0.333 62(15)	0.393 83(19)	H(2A)	0.574 5(25)	0.097 3(20)	0.312 0(24)
B(10)	0.991 78(19)	0.349 39(15)	0.455 67(18)	H(2B)	0.509(3)	0.196 3(18)	0.314 2(25)
B(11)	0.910 15(18)	0.245 61(14)	0.441 74(16)	H(2C)	0.548 1(23)	0.172 7(20)	0.210(3)
B(12)	1.070 09(19)	0.243 42(14)	0.471 58(17)				

general, less deformed from planarity than the upper C_2B_3 face[4]], and it is significant that H(35) is only 2.82 Å from the best (least-squares) plane through the C(11)–C(16) ring. In addition, the phenyl group is twisted by *ca.* 9.0° about the C(1)–C(11) bond such that C(16) is at a higher elevation than C(12). Presumably this twist is the result of reduction of close non-bonded contacts H(16)···H(4) and H(12)···H(2), 2.12(4) and 2.22(3) Å respectively, in the observed structure. The best plane through the indenyl ligand makes a dihedral angle of *ca.* 7.4° with the lower B_5 belt, but this overall angle includes both a sideways twist of *ca.* 5.1° [C(35) more elevated than C(38)] and an upward tilt of *ca.* 4.7° [C(36) more elevated than C(34)], both of which are attributable to the presence of the phenyl substituent on C(1) (equivalent twist and tilt angles in unsubstituted **1** are *ca.* 3.7 and *ca.* 0.6° respectively).

Table 8 summarises the essential slip and fold parameters[1,4] for compounds **1**–**4**. In each molecule the metal-bonded C_2B_3 face of the carbaborane ligand is envelope folded across the B(4)···B(7) vector in the same sense, and, as expected, there is no substantial slip of the d^6 metal atom across this face. In contrast, the cobalt atom is consistently and significantly further from C(34) and C(39) than from C(31), C(32) and C(33), resulting in Δ^h parameters of the order of 0.1 Å. The indenyl ligands are still, however, formally η^5-bonded to metal, *cf.* Δ^h *ca.* 0.7–0.8 Å for formally η^3-indenyl ligands.[17] Partial localisation of double-bond character in the C(35)–C(36) and C(37)–C(38)

connectivities of all three compounds is apparent from the data given in Table 7.

In compound **3** a single CH_2OMe group is substituted at C(1). Again, the observed molecular conformation is cisoid (Fig. 3). Unexpectedly the ether oxygen atom lies above the metal-bonded C_2B_3 carbaborane face, but this may be traced to an intramolecular interligand hydrogen bond [O(1)···H(33) 2.544(22) Å; H(33)···O(1)–C(11) 112.7(5), H(33)···O(1)–C(12) 122.7(5)°]. The indenyl ligand in **3** is twisted and tilted similarly to that in **2** (*ca.* 6.5 and 5.4° respectively) making an overall dihedral angle of *ca.* 8.1° with the reference B_5 plane. The closest H(ether)···H(indenyl) contact in **3** is 2.51(3) Å, between H(112) and H(35).

In contrast to the cisoid conformations of compounds **1**–**3**, the key feature of the structure of **4**, which contains two C-substituted CH_2OMe groups, is that the ring-junction atoms of the indenyl ligand are rotated by *ca.* 72° from their positions in **1**–**3** to lie above B(7) (Fig. 4). Electronically this is the second best staggered conformation of **1**,[1] and presumably it arises in **4** as the result of steric crowding between the upwardly directed ether functions and the indenyl six-membered ring. It is of interest that in the recently reported compound $[(\eta\text{-}C_9H_7)Fe(Et_2C_2B_4H_4)Ni(\eta\text{-}C_5Me_5)]$,[18] in which the ethyl substituents on the eight-membered carbadimetallaborane are *not* substantially inclined towards the indenyl ligand, the indenyl-cage conformation appears to be *cis*. In **4** both ether oxygen atoms lie

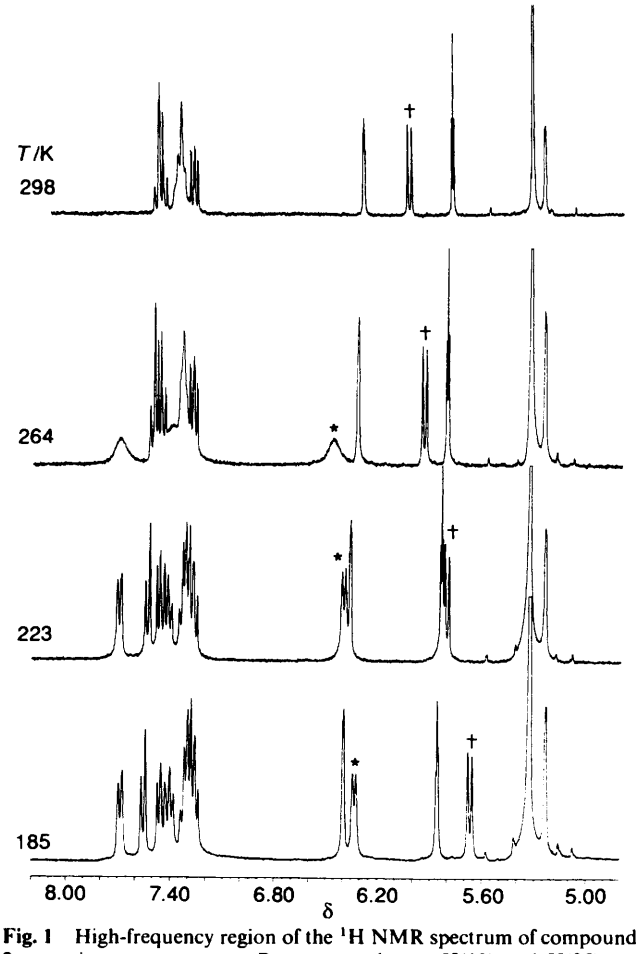

Fig. 1 High-frequency region of the ^1H NMR spectrum of compound **2** at various temperatures. Resonances due to H(12) and H(35) are marked * and † respectively

Table 5 Parameters used in EHMO calculations

Parameter	Value	Parameter	Value
B–B	1.75 Å	B–C	1.75 Å
C–C(cage)	1.75 Å	C–C(hydrocarbon)	1.40 Å
Co–C	2.05 Å	Co–B	2.05 Å
B–H	1.20 Å	C–H(cage)	1.20 Å
C–H(hydrocarbon)	1.08 Å	C–C(methyl)	1.54 Å
Co–C–C–H(methyl)	0°	Co–C–C–H(phenyl)	90°

α is the dihedral angle [centre of C(34)–C(39) bond]–[centroid of C(31)C(32)C(33)C(34)C(39) ring]–[centroid of C(1)C(2)B(7)B(8)B(4) ring]–[centre of C(1)–C(2) bond], where 0° is *cis*-eclipsed, 180° is *trans*-staggered, and 72° has C(34) eclipsing C(2). Ether groups modelled by CH_3. Thus models **I** and **II** are idealised representations of compounds **1** and **2** respectively, whilst **III** and **IV**, 1-Me-3-$(\eta\text{-}C_9H_7)$-3,1,2-*closo*-$CoC_2B_9H_{10}$ and 1,2-Me_2-3-$(\eta\text{-}C_9H_7)$-3,1,2-*closo*-$CoC_2B_9H_9$, are models for **3** and **4** respectively.

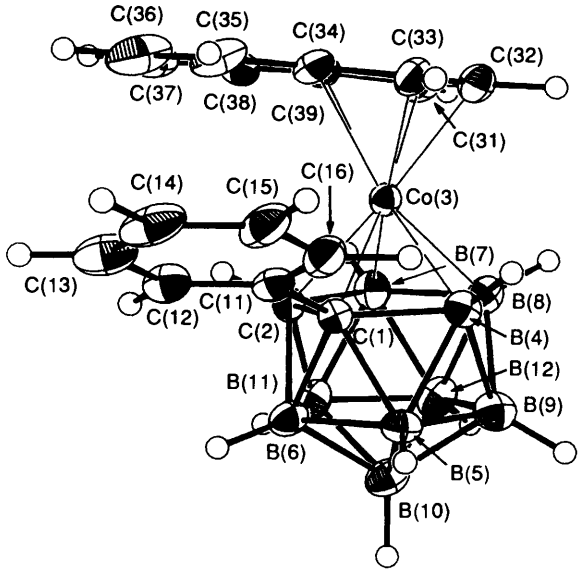

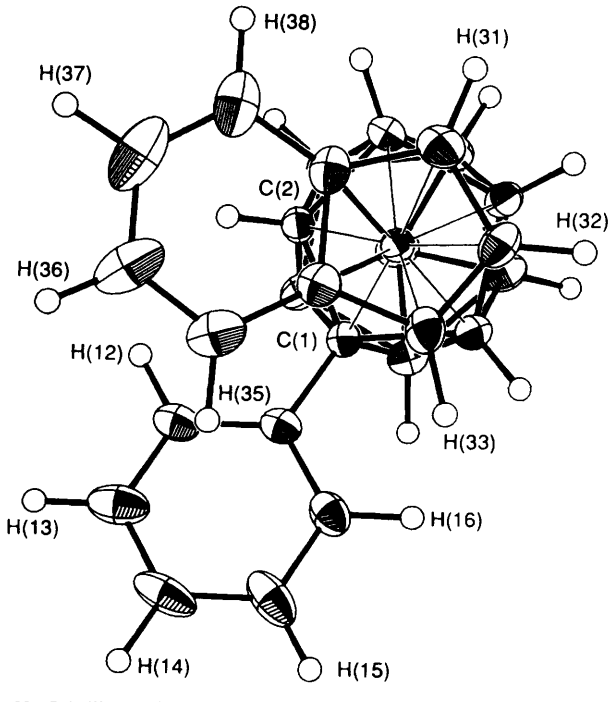

Fig. 2 Perspective and plan views of $[1\text{-Ph-3-}(\eta\text{-}C_9H_7)\text{-3,1,2-}closo\text{-}CoC_2B_9H_{10}]$ **2**, illustrating the numbering system for non-H atoms. Thermal ellipsoids are drawn at the 50% probability level except for H atoms which have an artificial radius of 0.1 Å for clarity

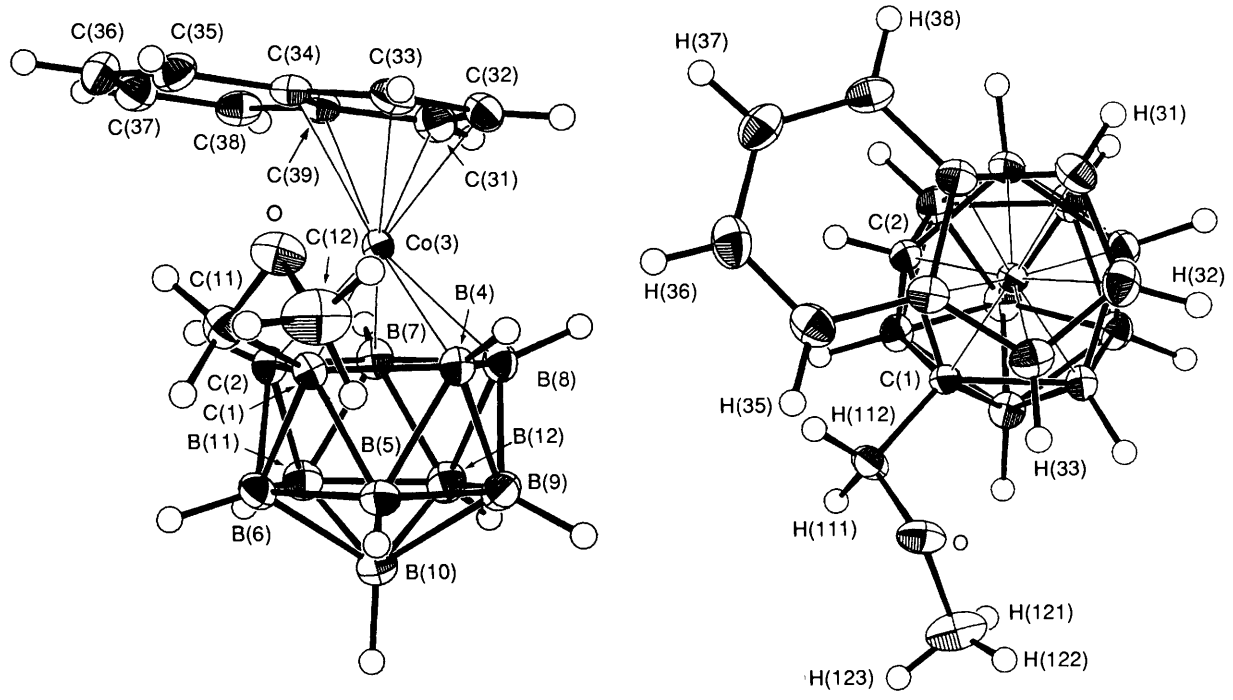

Fig. 3 Perspective and plan views of [1-(CH_2OMe)-3-(η-C_9H_7)-3,1,2-*closo*-$CoC_2B_9H_{10}$] **3**, with thermal ellipsoids drawn as in Fig. 2

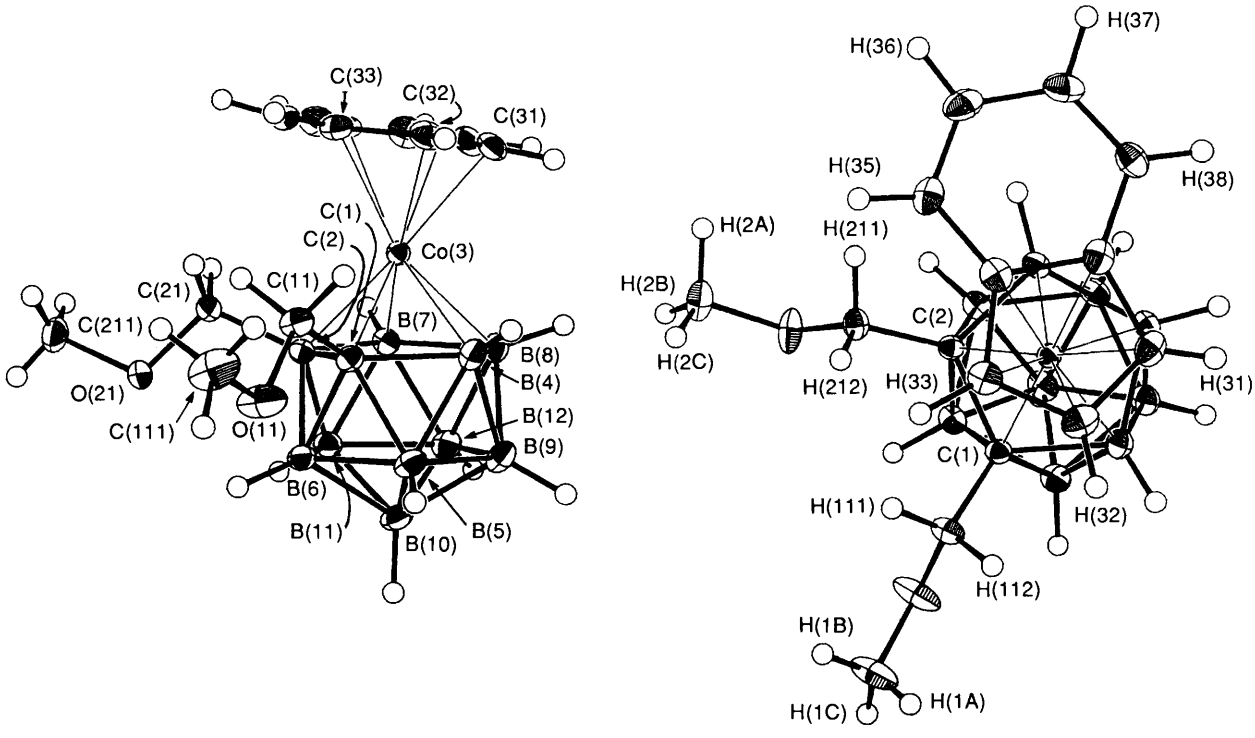

Fig. 4 Perspective and plan views of [1,2-(CH_2OMe)$_2$-3-(η-C_9H_7)-3,1,2-*closo*-$CoC_2B_9H_9$] **4**

below the metal-bonded C_2B_3 face, as the result of which both sets of methylene hydrogen atoms are directed upwards. Closest H(ether) ··· H(indenyl) contacts are H(112) ··· H(32) 2.51(3) and H(211) ··· H(35) 2.53(3) Å, consistent with the observation that the indenyl ligand in **4** is substantially twisted (*ca.* 6.7°), but barely tilted (*ca.* 1.4°).

The observed conformational preferences in compounds **2**–**4** are broadly supported by the results of EHMO calculations on the model compounds **II**–**IV**, constructed as detailed in Table 5. In Fig. 5 we present plots of relative energy *versus* α for **I**–**IV** drawn to a common scale. Although the plot for **I** (model of **1**) appears essentially flat when drawn with the vertical scale adopted in Fig. 5 we have previously[1] analysed in detail all its minima and maxima, the former occurring when the conformation between the two five-membered rings bonded to the metal is staggered (α = 36, 108 and 180°), the latter when it is eclipsed (α = 0, 72 and 144°). Moreover, we have fully discussed the preference for the global minimum (α = 36°) in terms of optimum metal–ligand bonding, and have shown that this conformation is observed experimentally in the structure of **1**.[1]

Our purpose in undertaking EHMO calculations on **II**–**IV**

was two-fold: first to determine whether the conformations observed crystallographically were predicted to be energetically favourable, and secondly to establish some rough idea of the relative heights of the barriers to full rotation of the indenyl ligand in compounds **2**–**4**, particularly in view of the interesting low-temperature NMR results already discussed. Fig. 5 clearly shows that the potential-energy plots for **II**–**IV** each consist of undulating valleys and a single large maximum. The frequency of undulation in the valleys is *ca.* 72°, corresponding to a series of staggered–eclipsed–staggered–eclipsed, *etc.*, conformations in which there is little or no intramolecular crowding. As indicated by the arrows, the experimentally determined conformations each occur on or near the valley floor. Conversely, the global maxima for **II**–**IV** occur at conformations corresponding to maximum indenyl • • • (cage substituent) crowding, in the case of monosubstituted **II** and **III** at $\alpha = 324°$ and in disubstituted **IV** at $\alpha = 0°$.

Table 6 Chemical shifts and assignments in the high-frequency region of the ^{1}H NMR spectra of compound **2** at 298 and 185 K

	δ	
	298 K	185 K
H(31)	6.30	6.40
H(33)	5.79	5.85
H(34)	5.26	5.23
H(35)	6.04	5.66
H(36)	7.28	7.26
H(37)	7.46	7.44
H(38)	7.50	7.55
H(13)	7.3–7.4	*ca.* 7.3
H(14)		*ca.* 7.3
H(15)		7.40
H(12)	—	6.34
H(16)	—	7.68

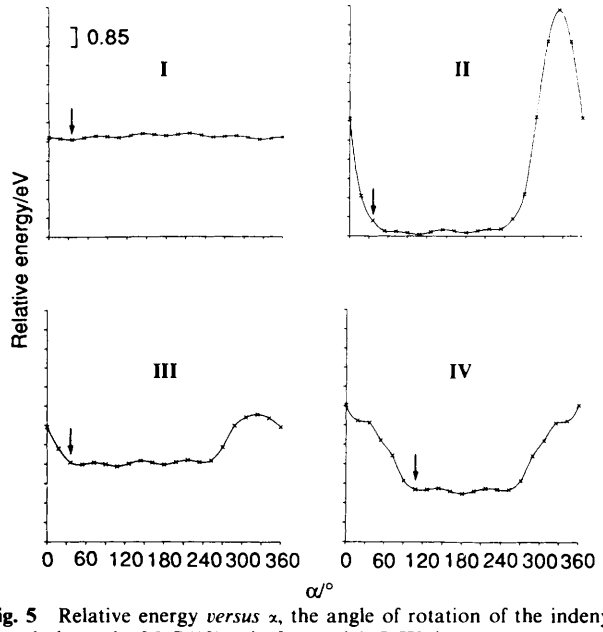

Fig. 5 Relative energy *versus* α, the angle of rotation of the indenyl ligand about the M–B(10) axis, for models **I**–**IV** drawn to a common scale. Arrows indicate the experimentally determined conformations

Table 7 Comparison of selected internuclear distances (Å) and interbond angles (°) in compounds **2**–**4**

	2	**3**	**4**		**2**	**3**	**4**
C(1)–C(2)	1.651(5)	1.659(3)	1.6822(24)	B(6)–B(10)	1.744(6)	1.768(3)	1.768(3)
C(1)–Co(3)	2.047(3)	2.0420(19)	2.0313(18)	B(6)–B(11)	1.752(6)	1.770(3)	1.770(3)
C(1)–B(4)	1.719(5)	1.720(3)	1.739(3)	B(7)–B(8)	1.785(6)	1.797(3)	1.808(3)
C(1)–B(5)	1.719(5)	1.708(3)	1.708(3)	B(7)–B(11)	1.783(6)	1.783(3)	1.785(3)
C(1)–B(6)	1.734(5)	1.731(3)	1.735(3)	B(7)–B(12)	1.775(6)	1.772(3)	1.774(3)
C(2)–Co(3)	2.008(4)	2.0025(20)	2.0412(16)	B(8)–B(9)	1.787(6)	1.785(3)	1.779(3)
C(2)–B(6)	1.724(5)	1.724(3)	1.724(3)	B(8)–B(12)	1.791(6)	1.791(3)	1.782(3)
C(2)–B(7)	1.707(6)	1.713(3)	1.736(3)	B(9)–B(10)	1.785(6)	1.780(3)	1.782(3)
C(2)–B(11)	1.702(6)	1.699(3)	1.694(3)	B(9)–B(12)	1.791(6)	1.790(3)	1.783(3)
Co(3)–B(4)	2.054(4)	2.0671(21)	2.0589(21)	B(10)–B(11)	1.764(6)	1.780(3)	1.778(3)
Co(3)–B(7)	2.065(4)	2.0690(22)	2.0534(21)	B(10)–B(12)	1.776(6)	1.772(3)	1.790(3)
Co(3)–B(8)	2.075(4)	2.0856(21)	2.1031(20)	B(11)–B(12)	1.766(6)	1.771(3)	1.779(3)
Co(3)–C(33)	2.064(4)	2.0685(19)	2.0818(18)	C(33)–C(32)	1.412(5)	1.402(3)	1.417(3)
Co(3)–C(32)	2.023(4)	2.0294(22)	2.0596(21)	C(33)–C(34)	1.436(5)	1.433(3)	1.4359(25)
Co(3)–C(31)	2.026(4)	2.0161(22)	2.0319(19)	C(32)–C(31)	1.420(5)	1.421(3)	1.409(3)
Co(3)–C(39)	2.133(4)	2.1198(19)	2.1107(18)	C(31)–C(39)	1.429(5)	1.433(3)	1.438(3)
Co(3)–C(34)	2.150(4)	2.1511(18)	2.1506(17)	C(39)–C(38)	1.419(6)	1.425(3)	1.429(3)
B(4)–B(5)	1.790(6)	1.788(3)	1.792(3)	C(39)–C(34)	1.434(5)	1.439(3)	1.4352(25)
B(4)–B(8)	1.811(6)	1.824(3)	1.798(3)	C(38)–C(37)	1.375(7)	1.351(3)	1.353(3)
B(4)–B(9)	1.769(6)	1.780(3)	1.790(3)	C(37)–C(36)	1.404(7)	1.420(3)	1.427(3)
B(5)–B(6)	1.754(6)	1.760(3)	1.772(3)	C(36)–C(35)	1.361(7)	1.362(3)	1.365(3)
B(5)–B(9)	1.770(6)	1.768(3)	1.776(3)	C(35)–C(34)	1.414(6)	1.427(3)	1.415(3)
B(5)–B(10)	1.776(6)	1.769(3)	1.779(3)				
C(1)–Co(3)–C(2)	48.04(14)	48.43(8)	48.79(7)	C(33)–C(34)–C(35)	131.4(3)	132.58(17)	132.59(17)
C(2)–Co(3)–B(7)	49.52(16)	49.74(8)	50.16(7)	C(33)–C(34)–C(39)	107.6(3)	107.56(16)	107.31(15)
B(7)–Co(3)–B(8)	51.08(17)	51.26(8)	51.55(8)	C(39)–C(34)–C(35)	121.0(3)	119.85(17)	120.09(16)
B(8)–Co(3)–B(4)	52.05(17)	52.10(8)	51.17(8)	C(34)–C(35)–C(36)	117.1(4)	118.20(19)	118.34(17)
B(4)–Co(3)–C(1)	49.55(15)	49.49(8)	50.31(8)	C(35)–C(36)–C(37)	122.6(5)	121.55(20)	121.56(18)
C(31)–Co(3)–C(32)	41.06(15)	41.12(9)	40.27(8)	C(36)–C(37)–C(38)	122.1(5)	122.38(20)	121.97(18)
C(32)–Co(3)–C(33)	40.41(15)	40.00(8)	40.01(8)	C(37)–C(38)–C(39)	117.2(4)	118.28(18)	118.10(18)
C(33)–Co(3)–C(34)	39.79(14)	39.64(7)	39.62(7)	C(38)–C(39)–C(31)	132.2(4)	133.04(18)	132.40(17)
C(34)–Co(3)–C(39)	39.11(14)	39.37(7)	39.35(7)	C(38)–C(39)–C(34)	119.9(3)	119.73(17)	119.94(16)
C(39)–Co(3)–C(31)	40.11(15)	40.46(8)	40.56(7)	C(31)–C(39)–C(34)	107.8(3)	107.20(16)	107.66(15)
C(31)–C(32)–C(33)	108.9(3)	108.77(19)	108.87(17)	C(39)–C(31)–C(32)	107.8(3)	107.99(18)	107.97(16)
C(32)–C(33)–C(34)	107.8(3)	108.33(17)	108.02(16)				

Table 8 Slip and fold parameters[a] for compounds **1**–**4**

	1[b]	2	3	4
φ^p/°	0.49	0.42	0.46	1.23
θ^p/°	2.35	1.73	2.36	2.37
Δ^p/Å	0.028	0.035	0.026	0.013
Δ^h/Å	0.089	0.118	0.114	0.082

[a] For definition see refs. 1 and 4. [b] α Form, see ref. 1.

For models **III** and **IV** the height of the potential barriers appears to be proportional to the number of ether substituents. However, it is clear that the greatest barrier to indenyl rotation (*ca.* 10 eV) is calculated for the monophenyl model **II**. Although this theoretical barrier is almost certainly overestimated relative to the experimental barrier in the real molecule **2** (since a simple rigid-rotor model is used in the calculations) it may nevertheless be highly significant that the solution fluctionality of **2** may be arrested by cooling, whilst that of **4** has not been.

Acknowledgements

We thank the Department of Education for Northern Ireland for support (to Z. G. L.) and the Callery Chemical Company for a generous gift of decaborane.

References

1 Part 1, D. E. Smith and A. J. Welch, *Organometallics*, 1986, **5**, 760.
2 M. F. Hawthorne, D. C. Young, T. D. Andrews, D. V. Howe, R. L. Pilling, A. D. Pitts, M. Reintjes, L. F. Warren and P. A. Wegner, *J. Am. Chem. Soc.*, 1968, **90**, 879.
3 See, for example, R. M. Wing, *J. Am. Chem. Soc.*, 1970, **92**, 1187; C. Glidewell, *J. Organomet. Chem.*, 1975, **102**, 339; D. M. P. Mingos and M. I. Forsyth, *J. Organomet. Chem.*, 1978, **146**, C37; H. M. Colquhoun, T. J. Greenhough and M. G. H. Wallbridge, *J. Chem. Soc., Dalton Trans.*, 1978, 303 and refs. therein.
4 D. M. P. Mingos, M. I. Forsyth and A. J. Welch, *J. Chem. Soc., Dalton Trans.*, 1978, 1363.
5 See, for example, C. White and R. J. Mawby, *Inorg. Chim. Acta*, 1970, **4**, 441; S. R. Allen, P. K. Baker, S. G. Barnes, M. Bottrill, M. Green, A. G. Orpen, I. D. Williams and A. J. Welch, *J. Chem. Soc., Dalton Trans.*, 1983, 927; M. E. Rerek and F. Basolo, *J. Am. Chem. Soc.*, 1984, **106**, 5908; L.-N. Ji, M. E. Rerek and F. Basolo, *Organometallics*, 1984, **3**, 740; J. W. Faller, R. H. Crabtree and A. Habib, *Organometallics*, 1985, **4**, 929; N. N. Turaki, J. M. Huggins and L. Lebioda, *Inorg. Chem.*, 1988, **27**, 424; S. A. Westcott, A. K. Kakkar, G. Stringer, N. J. Taylor and T. B. Marder, *J. Organomet. Chem.*, 1990, **394**, 777, and refs therein.
6 B. D. Reid and A. J. Welch, unpublished work.
7 K. F. Shaw and A. J. Welch, *Polyhedron*, in the press.
8 H. M. Colquhoun, T. J. Greenhough and M. G. H. Wallbridge, *J. Chem. Soc., Chem. Commun.*, 1977, 737; P. Jutzi, D. Wegener and M. B. Hursthouse, *Chem. Ber.*, 1991, **124**, 295.
9 CADABS, R. O. Gould and D. E. Smith, University of Edinburgh, 1986.
10 SHELX86, G. M. Sheldrick, University of Göttingen, 1986.
11 SHELX76, G. M. Sheldrick, University of Cambridge, 1976.
12 DIFABS, N. G. Walker and D. Stuart, *Acta Crystallogr., Sect. A*, 1983, **39**, 158.
13 CALC, R. O. Gould and P. Taylor, University of Edinburgh, 1986.
14 EASYORTEP, P. D. Mallinson and K. W. Muir, *J. Appl. Crystallogr.*, 1985, **18**, 51.
15 ICON8, J. Howell, A. Rossi, D. Wallace, K. Haraki and R. Hoffmann, Quantum Chemistry Program Exchange, University of Indiana, 1977, no. 344.
16 J. H. Ammeter, H.-B. Burgi, J. C. Thibeault and R. Hoffmann, *J. Am. Chem. Soc.*, 1978, **100**, 3686.
17 A. W. Nesmeyanov, N. A. Ustynyuk, L. G. Makarova, V. G. Andrianov, Yu. T. Struchov, S. Andrae, Yu. A. Ustynyuk and S. G. Malyugina, *J. Organomet. Chem.*, 1978, **159**, 189; J. S. Merola, R.-T. Kacmarcik and D. Van Engen, *J. Am. Chem. Soc.*, 1986, **108**, 329; T. C. Forschner, A. R. Cutler and R. K. Kullnig, *Organometallics*, 1987, **6**, 889.
18 A. Fessenbecker, M. Stephen, R. N. Grimes, H. Pritzkow, U. Zenneck and W. Siebert, *J. Am. Chem. Soc.*, 1991, **113**, 3061.

Received 2nd *July* 1991; *Paper* 1/03312C